Korean J. Chem. Eng., 33(12), 3529-3540 (2016)
DOI: 10.1007/s11814-016-0218-z

pISSN: 0256-1115
eISSN: 1975-7220

Enhancing removal and recovery of magnesium from aqueous solutions by using modified zeolite and bentonite and process optimization

Mohammad Amin Alaei Shahmirzadi*, Seyed Saeid Hosseini*,†, and Nicolas Raymond Tan**

*Department of Chemical Engineering, Tarbiat Modares University, Tehran 14115-114, Iran
**Research & Development Department, HOSSTECH Group, Singapore 528844, Singapore
(*Received 14 April 2016 • accepted 30 July 2016*)

Abstract−Natural and modified zeolite and bentonite are investigated and characterized for extraction of magnesium from aqueous solutions. Magnesium removals as high as 85.21% and 81.73% were achieved by calcined bentonite and microwave radiated zeolite, respectively. The effects of various operational parameters were studied and optimized using selected isotherms. Maximum Mg (II) adsorption capacities of 26.24 and 35.67 $mg \cdot g^{-1}$ were obtained on pristine and calcined bentonites, respectively. Thermodynamic studies suggest that magnesium adsorption on natural bentonite is spontaneous and endothermic (9.13 $kj \cdot mol^{-1}$). Also, desorption study of natural bentonite demonstrates that HNO_3 is more effective by offering 89.11% desorption than other desorptive counterparts.

Keywords: Adsorption, Magnesium, Inorganic Adsorbents, Thermal Modification, Acid Treatment, Removal Efficiency

INTRODUCTION

Desalination is widely accepted as a viable technology for meeting long-term demands for drinking, agricultural and industrial waters in arid regions [1]. In fact, water scarcity is considered as one of the most important concerns in Iran as well as other countries in the Middle East in the present and foreseeable future [2]. This is because the presence of heavy metal, nitrate, calcium, magnesium and other minerals is not in favorable levels in most of the water resources and this adds into the complexities involved [3,4].

Removal and recovery of magnesium from water has several advantages. Calcium and magnesium are recognized as the main species causing the formation of scales leading to decrement in heat transfer in boilers and potentially malfunction of pipelines. Also, the high concentration of magnesium tends to give a bitter taste to the water [3,5]. On the other hand, seawater desalination using RO is the most widespread technology in the world [6]. In RO desalination plants, hardness removal is necessary for prevention of membrane scaling, which adversely affects the process performance and overall treatment costs [7]. Discharge of the brine produced by the RO desalination process results in many environmental adverse effects, due to the high concentrations of metals and salts. Recovery and removal of elements from RO brine would decrease environmental impacts and create economic gains in the production of valuable metals [8]. From another aspect, magnesium is listed as an element with high economical value [9]. Extraction of lithium from salt lake brine and seawater is one of the main sources of lithium production. Lithium has similar ionic size as magnesium, making it difficult to separate lithium from magnesium. Magnesium ions prohibit lithium chloride formation, which is the first step in the production of lithium carbonate desired product. Removal of magnesium decreases the Mg/Li ratio in brine and facilitates lithium extraction and makes it economical.

Several technologies have been used for magnesium removal. Precipitation using lime and/or soda is an established technique used for extraction of magnesium from aqueous solutions. However, the main drawback is generation of large volumes of sludge, which usually results in dewatering and disposal problems in addition to the need for re-carbonation of the softened water [3,10]. Alternatively, ion exchange resins have been widely used for removal of calcium and magnesium ions. Ion exchange resins offer advantages such as high capacity and fast kinetics [11-13]. On the other hand, they must be regenerated by chemical reagents often causing subsequent pollutions in addition to being expensive especially for large scale applications [10].

In recent years, some other techniques such as micellar enhanced ultrafiltration (MEUF) [14], polymer enhanced ultrafiltration (PEUF) [15], reverse osmosis [15], nanofiltration [16], electrodialysis [17], electrochemical treatment [18] and adsorption [1,5,17-28] have emerged for removal and recovery of ions from aqueous solutions. Several types of adsorbents have been investigated for their ion removal efficiency. Recently, unmodified and functional nanomaterials have been promising for recovery of metal ions [29-33]. Especially in case of magnesium, Tofighy et al. [34] investigated water softening using oxidized carbon nanotube (CNT) sheets. The results showed that oxidized CNTs were effective for separation of calcium and magnesium. However, CNTs may have drawbacks, such as the difficulty of separation from treated water and degree of toxicity and, as a result, their safety aspects remain controversial. Therefore, economical water softening without CNT leakage into water is preferable. Fly ash is also used as low-cost adsorbent for treating the salty solution. The results revealed that the removal efficiency of magnesium was as low as 29%. Activated carbon has been evaluated for water softening despite its relatively high price

†To whom correspondence should be addressed.
E-mail: saeid.hosseini@modares.ac.ir, seyedsaeidhosseini@gmail.com

[35]. Among the low-cost adsorbents [27], natural clay minerals (e.g., bentonite) [36,37] and zeolite [38,39] have been examined for adsorption of heavy metals and molecular species from various water streams. Utilization of inorganic adsorbents has many advantages such as less environmental impact and toxicity, low-cost in addition to abundance in most soils. Bentonite is one of the main clay minerals and is mostly composed of montmorillonite and aluminosilicate [35]. Bentonites are very valuable because of their particular sorptive properties originating from their high surface area. This property enables high tendency of bentonites to adsorb water in the interlayer sites [40]. Moreover, zeolites are crystalline aluminosilicates, structurally based on tetrahedral SiO_4 and AlO_4 units, connected by shared oxygen atoms forming interconnected cages and channels [2]. Silicon is tetravalent and aluminum is trivalent, and hence the structure of zeolite is negatively charged [39]. Zeolites are capable of exchanging ions, and the negative charge of zeolite causes their high tendency towards cations (versus anions) and non-polar organic molecules [41].

Various modification methods such as thermal treatment, acid treatment as well as surfactant modification can be employed for improving the characteristics and performance of adsorbents. It is demonstrated that thermal treatment of zeolite and bentonite changes their physicochemical and textural properties [40,42,43]. Moreover, acid treatment has been used for modification of mineral adsorbents and improving the chemical and structural properties of natural zeolite and bentonite. [39,44]. It is also shown that acid treatment could result in modified mesoporosity, textural and structural characteristics of bentonite [44].

As reported, the high prices, low efficiency, and adverse environmental impacts are the main drawbacks attributed to utilization of adsorbents for water softening and magnesium removal from aqueous solutions. Based upon the vast experiences gained over the years in our research group on various separation processes [45-54], the impetus for the present research study was to explore the characteristics and performance of efficient, environmental friendly, low-cost and less toxic adsorbent (zeolite and bentonite) for this purpose. The effects of various modification techniques including acid and thermal (by calcination and microwave radiation) treatments of adsorbents on the separation performance were investigated and analyzed. To the best of our knowledge, it is for the first time that capability of bentonite for removal of magnesium from aqueous solutions is being investigated and reported. Another novelty of the present study is the employment of thermal treatments for improving the characteristics and adsorption performance of zeolite and bentonite. Thermal treatment by microwave has not been applied for this purpose before. Furthermore, the effects of several processes and operational parameters such as the mass of adsorbent, the initial concentration of magnesium, contact time, pH, temperature, agitation speed, and particle size were investigated on the adsorption efficiency of bentonite as the model adsorbent. Adsorption isotherms were plotted, analyzed and compared with respect to the well-established Langmuir, Freundlich, and Dubinin-Raduskevich (D-R) models.

MATERIALS AND METHODS

1. Materials

Natural zeolite and bentonite adsorbents were provided in the powder form by a local mining plant in Semnan (Negin Powder Co.), Iran. Bentonite powders were provided in four range of particle sizes ranging from 88 to 354 μm. Solutions of Mg (II) in various compositions were prepared by dissolving prescribed amounts of $MgSO_4 \cdot 7H_2O$ in double distilled water and stirring at room temperature until obtaining homogeneous solutions. The pH of solutions adjusted using 0.1 M H_2SO_4 and 0.1 M NaOH. All other chemical reagents used in this work were of analytical grade and purchased from Merck (Germany).

2. Characterizations

Zeolite and bentonite powders were characterized by various instruments. The chemical composition of both adsorbents was characterized by X-ray florescence (XRF; Philips PW 2404). Surface microstructure and morphology of adsorbents were characterized using scanning electron microscopy (SEM) (Philips XL30 and ZEISS-DSM 960A). The crystallinity of the powders was examined using a Bruker D8 ADVANCE X-ray diffractometer (XRD) employing Cu Kα radiation.

3. Acid Treatment Procedures

Acid treatment of zeolite powders was carried out using a glassy flat bottom flask placed onto a Wisd MSH-D hotplate magnetic stirrer according to the following procedure. 30 grams of zeolite

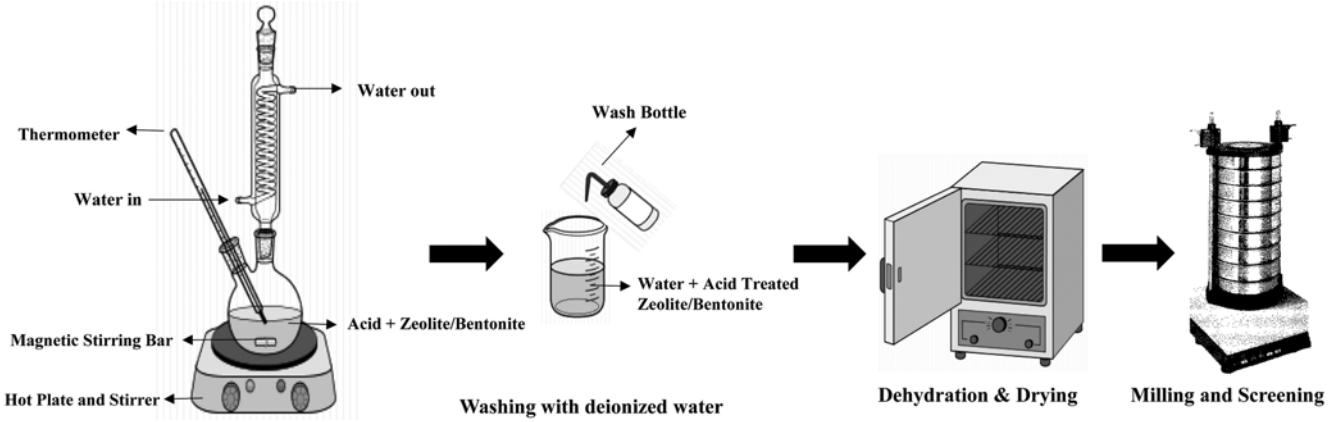

Fig. 1. Schematic of procedures involved in acid treatment of zeolite and bentonite.

was added into 100 mL of 1 N HCl solution and then stirred for 3 hrs. On the other hand, acid treatment of bentonite powders involved using a glassy round-bottom flask reactor with a reflux condenser. The reactor was placed onto a Wisd MSH-D hotplate magnetic stirrer. 20 grams of raw bentonite was added into 250 ml of 5 N HCl solution, stirred well and maintained at boiling temperature (~378 K) for 3 hrs. Upon preparation, individual suspensions were then cooled naturally before filtration and then washed with deionized water until the pH of filtrates reached a constant value (~pH 7), ensuring complete residual acid removal. The resultant slurries were dehydrated by drying at 80 °C for 24 hrs and then milled and screened using mesh sieve #170 (88 μm). The final powders were stored in a desiccator until use. The adopted procedures are shown schematically in Fig. 1.

4. Thermal Treatment Procedure

4-1. Calcination

Prescribed amounts of zeolite and bentonite powders were subjected to calcination at various temperatures of 100 °C, 400 °C and 700 °C using an atmospheric muffle furnace. The period of calcination was 24 hrs for all the samples, then samples were removed from the furnace and cooled naturally over a silica gel bed to avoid adsorption of any moisture. Calcined samples were then milled and screened using mesh sieve # 170 (88 μm). The calcined powders were finally stored in a desiccator until use.

4-2. Microwave Radiation

Prescribed amounts of zeolite and bentonite powders were exposed to microwave radiation at the frequency of 2.45 GHz (900 Watt) for 5, 15 and 30 min in an industrial microwave oven (Panasonic Inc.). The samples were then allowed to cool naturally over a silica gel bed to avoid adsorption of any moisture. The final powders were then milled and screened using mesh sieve # 170 (88 μm). The powders were finally stored in a desiccator until use.

5. Adsorption Experiments

Specified quantities of zeolite and bentonite powders were added individually into 50 ml solutions containing known concentration (in the range of 250-550 $mg \cdot L^{-1}$) of Mg (II) while being stirred on a thermostated shaker (Heidolph unimax). Samples then underwent rigorous shaking at various speeds between 50-300 rpm for 5 to 120 min time intervals at 20, 30, 40, 50, and 60 °C. Adsorbents were separated from the solution by centrifugation for 5 min at 3,000 rpm using ShimiFan ultracentrifuge (Model: CE-148). The concentration of Mg (II) ions in the solutions was measured before and after the process by using flame atomic absorption spectrophotometer (FAAS).

The ion removal efficiency (%) and distribution constant (K_d) were calculated using following equations, respectively:

$$RE = \frac{C_0 - C_e}{C_0} \times 100 \quad (1)$$

$$K_d = \frac{C_0 - C_e}{C_0} \times \frac{V}{m} \quad (2)$$

where C_0 ($mg \cdot L^{-1}$) and C_e ($mg \cdot L^{-1}$) are the concentrations of the Mg (II) ion in the solutions before and after the adsorption, respectively. V and m are the volume of liquid phase (mL) and the weight of the adsorbent (g), respectively.

The adsorption capacity of adsorbents for Mg (II) was calculated using the following equation:

$$q_e = C_0 - C_e \times \frac{V}{m} \quad (3)$$

where q_e is the equilibrium concentration of Mg (II) on the adsorbent (mg of ion per g of adsorbent). All the experiments were repeated at least twice to ensure reproducibility of the results with standard deviations in the range of ±5.0%. In the rest of the experiments, bentonite was selected as the model adsorbent to investigate the effects of several process parameters on the removal and recovery efficiency of Mg (II) ions.

6. Desorption and Regeneration

The regeneration characteristics were examined on bentonite powders using various solutions. For this purpose, 1 $g \cdot L^{-1}$ of loaded adsorbent was added into the individual bottles containing 50 ml of 1 M solution of NaOH, HNO_3, HCl and pure water before shaking at 200 rpm and 30 °C for 60 min. Solutions were finally separated from the solids by centrifugation (5 min at 3,000 rpm). The concentration of Mg (II) ions was measured before and after desorption experiments using flame atomic absorption spectrometer (FAAS).

RESULTS AND DISCUSSION

1. Characterization of Adsorbents

The physicochemical properties of adsorbents play essential role in their application, especially adsorption performance. Accordingly, the elemental compositions of the zeolite and bentonite were analyzed by XRF, and the ingredients including their percentage in the overall composition are reported in Table 1. Results indicate that silica and alumina are major constituents of both zeolite and bentonite. The percentage of SiO_2 in the structure of zeolite is more than in bentonite. These suggest that zeolite may have more interactions with metal ions than bentonite due to the presence of more negatively charged (Si-O) - in its chemical structure. In the case of bentonite, the high proportion of SiO_2 and Al_2O_3 indicates the presence of montmorillonite. Both zeolite and bentonite also contain the prevailing exchangeable cations, such as Na (I), K (I), and Ca (II), which can effectively play a role in the adsorption of magnesium ions.

Table 1. The chemical composition of natural zeolite and bentonite analyzed by means of XRF

Ingredient	Zeolite (w%)	Bentonite (w%)
SiO_2	69.28	65.53
Al_2O_3	10.43	10.44
Fe_2O_3	0.49	1.24
CaO	3.56	3.23
MgO	0.50	1.57
Na_2O	0.73	3.51
K_2O	1.27	1.31
SO_3	0.005	1.91
L.O.I	12.97	9.75

The X-ray diffraction (XRD) patterns for zeolite and bentonite are shown in Fig. 2. Data demonstrate that both zeolite and bentonite consisted primarily of clinoptilolite and montmorillonite, respectively. The structural morphology and surface characteristics of zeolite and bentonite are exhibited in Fig. 3. The SEM image of zeolite shows that it consists of crystalline laminar habits and con-

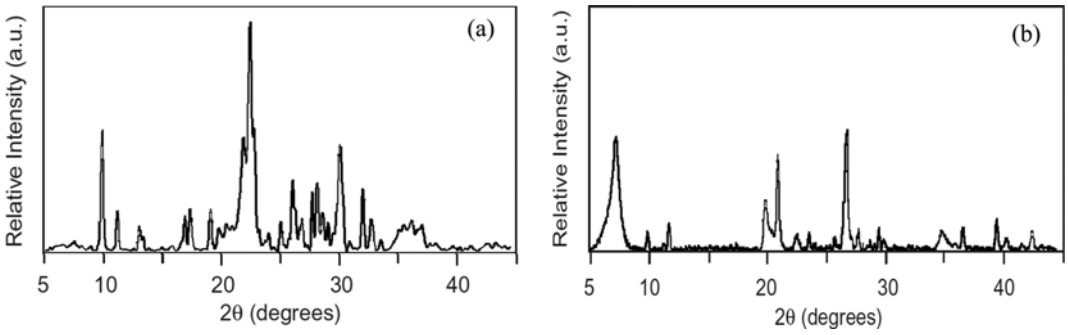

Fig. 2. X-ray diffraction patterns for natural (a) zeolite (b) bentonite [55].

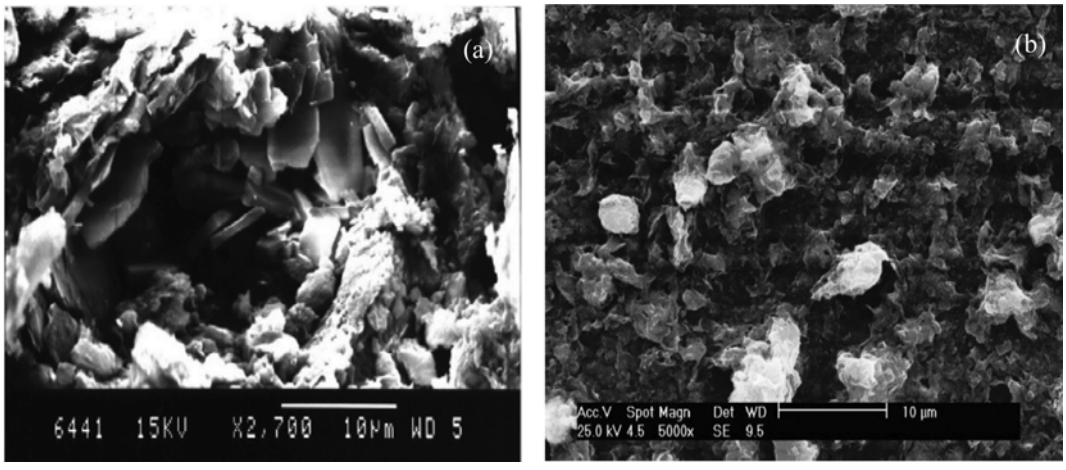

Fig. 3. SEM micrographs of (a) zeolite and (b) bentonite [56,57].

Table 2. Adsorption efficiency of zeolite and bentonite with respect to Mg (II) ions

Adsorbent	Code	Treatment type and condition	Mg (II) removal efficiency (%)
Zeolite	Z-N	Pristine (natural zeolite)	75.17
	Z-A	Acid treatment	77.65
	Z-C-100	Calcination at 100 °C	75.65
	Z-C-400	Calcination at 400 °C	79.58
	Z-C-700	Calcination at 700 °C	71.14
	Z-R-5	Radiation by microwave for 5 min	76.28
	Z-R-15	Radiation by microwave for 15 min	81.73
	Z-R-30	Radiation by microwave for 30 min	73.32
Bentonite	B-N	Pristine (natural bentonite)	69.47
	B-A	Acid treatment	82.43
	B-C-100	Calcination at 100 °C	70.34
	B-C-400	Calcination at 400 °C	85.21
	B-C-700	Calcination at 700 °C	62.56
	B-R-5	Radiation by microwave for 5 min	72.66
	B-R-15	Radiation by microwave for 15 min	84.33
	B-R-30	Radiation by microwave for 30 min	68.25

glomerates of compact crystals (Fig. 3(a)). On the other hand, the micrograph of bentonite reveals that it is composed of wavy flakes and honeycomb textures in the form of aggregates with porous surfaces. Surface properties of bentonite are specified on the basis of the montmorillonite content with its surface charges. Fig. 3(b) also reveals that there exist many micro and nano passages within the structure of bentonite. This possibly enables penetration and subsequently potential adsorption of selective ions on the active sites [55-57].

2. The Effect of Acid Treatment on the Performance of Adsorbents

The performance of adsorption of Mg (II) ions by natural and acid treated zeolite and bentonite was investigated, and the results are provided in Table 2. Based on the findings, essentially the removal efficiency of Mg (II) ions by natural zeolite was higher than natural bentonite. As shown in Table 1, SiO_4 and AlO_4 are the main components of zeolite and bentonite. Silicon is tetravalent and aluminum is trivalent, and hence the structure of both zeolite and bentonite are negatively charged. The negative surface charge of zeolite is greater than bentonite due to higher SiO_2/Al_2O_3 ratio and as a consequence, the Mg (II) adsorption on zeolite is more efficient. Acid treatment enhanced the adsorption efficiency of both adsorbents. The removal efficiency of Mg (II) ions by zeolite increased from 75.17% to 77.65% upon performing the acid treatment. This improvement could be attributed to various possible factors including the alteration of Si/Al ratio and chemical/structural properties, removal of impurities that block the pores, elimination of cations in order to change the adsorbent structure into H-form and eventually dealumination of zeolite [39,58]. Similarly, acid treatment also improved the adsorption efficiency of natural bentonite by almost 18%. As reported by Kul et al. [44], acid treatment causes the formation of fine pores in the solid particles, consequently leading to increased surface area and active sites for adsorption. The mechanisms of adsorption of Mg (II) ions onto pristine and acid-treated zeolite and bentonite are illustrated schematically in Fig. 4. In the case of pristine adsorbents, the Mg (II) ions in aqueous solution are exchanged with Na (I) and K (I), but in acid treated adsorbents, the adsorbent structure changes into H-form and the Mg (II) ions are exchanged with H (I).

3. The Effect of Thermal Treatments on the Performance of Adsorbents

Thermal treatment of natural zeolite and bentonite changed their composition, structure and separation efficiency. In this study, the influence of temperature (100-700 °C) and microwave exposure time (5-30 min) on the characteristics of adsorbents and their removal efficiency for Mg (II) ions was investigated, and the results are provided in Table 2. The findings indicate that heat treatment at 100 °C could not make considerable effects on the properties and performance of the adsorbents. However, ion removal efficiency of zeolite and bentonite calcined at 400 °C improved compared to their natural state by about 4% in case of zeolite and 15% in case of bentonite. This could be due to the improved increase in surface area as well as the release of impurities occupied active sites of the adsorbents [43]. The lower removal efficiency for thermally treated zeolite at 400 °C compared to bentonite can be attributed to partial fracture of zeolite crystals lead to the reduction of surface area. Further dehydration of active sites and removal of vapors entrapped within the structure of the adsorbents caused by the expansion of the structure at elevated temperature could be another factor playing a role. It has been demonstrated that calcination changes the textural properties of bentonite and improves its dispersion in aqueous solution and as a consequence facilitating the adsorption of Mg (II) ions [40]. Further increase in the calcination temperature to 700 °C had negative effect on the removal efficiency. These observations can be attributed to fracture of the crystal structure at the elevated temperature leading to a decrease in the specific surface area and adsorption capacity [40]. According to data in the literature, the thermal degradation of bentonite occurs at temperatures above 400 °C [40], while zeolite degrades at temperatures between 200-400 °C [43].

For both zeolite and bentonite exposed to radiation by microwave, removal efficiency increased with exposure time up to 15 min. Increase in adsorption capacity of microwave-treated minerals may be due to removal of water from the internal channels of natural zeolite and bentonite leaving the channels vacant and increasing adsorption sites [43]. The removal efficiency of both ad-

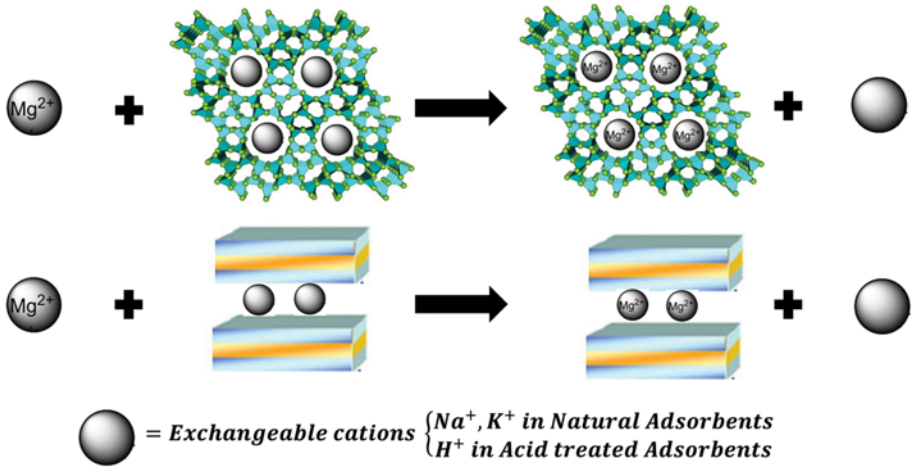

Fig. 4. The Mechanisms of adsorption of Mg (II) ions from aqueous solution on pristine (natural) and acid treated zeolite and bentonite.

sorbents decreased upon 30 mins exposure to microwave. Upon 30 mins exposure time, crystalline structure of both adsorbents collapses and surface area and hence removal efficiency decreases as also reported by Motsi et al. [43].

4. The Effect of Process Parameters on Process Efficiency

Due to its importance, the effect of several operational parameters on the adsorption characteristics was investigated and analyzed in the case of bentonite as the model adsorbent.

4-1. The Effect of Mass of Adsorbent

The effect of the mass of bentonite Mg (II) ion removal efficiency was investigated at five different adsorbent doses ranging from 0.5 to 4 g (Fig. 5). According to the findings, the removal efficiency of Mg (II) ions improved from 53.47% to 97.16% as the mass of adsorbent increased from 0.5 to 4.0 g, respectively. Interestingly, the improvement in the removal efficiency (~62%) was significant upon increasing mass of adsorbent from 0.5 g to 2 g. The findings could be attributed to the competition of metal ions in order to occupy limited adsorption sites at lower mass of bentonite. However, as mass of bentonite increased, greater surface area was available which exposed more vacant active adsorption site for binding of metal ions, resulting in higher adsorption of Mg (II) ions [59]. Further increase in the mass of adsorbent from 2 g to 4 g could only raise the removal efficiency by another 20%. In this range, the provided active sites are excess and more than required for metal ions in solution.

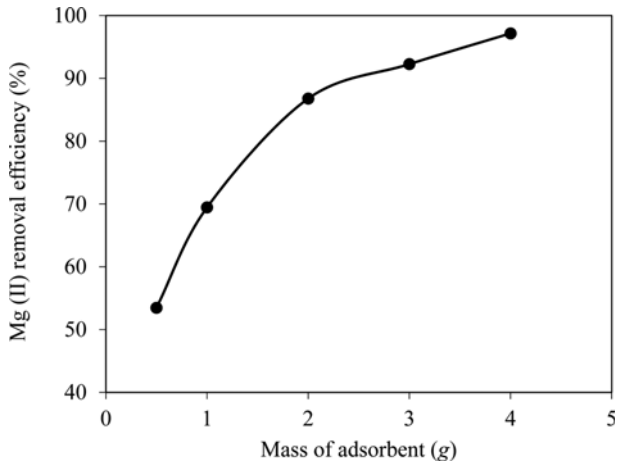

Fig. 5. Effect of mass of bentonite on removal efficiency of Mg (II) ions. Conditions: Mg (II) conc.: 250 mg·L^{-1}, bentonite particle size: 88 μm, pH: 4.00, V: 50 mL, t: 60 min, T: 30 °C, agitation speed: 100 rpm.

Bentonite turns into a sticky gel when in water [35]. This character is a limitation for application of high mass of bentonite for adsorption. Accordingly, the amount of bentonite in further experiments was limited to 1 g to prevent unwanted complexities in the analysis of the results.

4-2. The Effect of pH

The pH of aqueous solution is a significant operational parameter in adsorption of metal ions on adsorbents. Also, pH has a prominent effect on ionization degree and the surface charge of the adsorbent. As shown in Fig. 6(a), the removal efficiency of Mg (II) ions abruptly increased from 27.47% to 69.47% upon increase in pH from 2 to 4 and then gradually decreased at further pHs. The increase in Mg (II) adsorption on bentonite surface in the pH range between 2 and 4 can presumably be due to the partial hydrolysis of Mg (II) in aqueous solution. At pH<4, positively charged ions (Mg (II)) are attracted by columbic force between silica of bentonite and Mg (II). At pH>4, hydrolysis of Mg (II) gradually occurs and the negatively charged is formed, which leads to the decrease of adsorption of Mg (II) on bentonite due to electrostatic charge repulsion and decrease in the negative surface charge density [35,60]. The maximum adsorption of Mg (II) ions on bentonite was achieved at pH 4. Due to the highest adsorption of metal ions, further experiments were carried out at pH=4.

4-3. The Effect of Initial Ion Concentration

The effect of initial concentration of magnesium ions on the removal efficiency of bentonite was studied, and the results are shown in Fig. 6(b). The initial Mg (II) concentration was varied from 250 to 550 mg·L^{-1}. According to the findings, removal efficiency decreased from 73.29% to 57.25% in the low to medium (250 to 500 mg·L^{-1}) concentrations, which could be attributed to lower ratio of surface active sites to total magnesium ions. Hence, interaction between metal ions and adsorption sites present on the surface of bentonite particles was not efficient. However, at higher

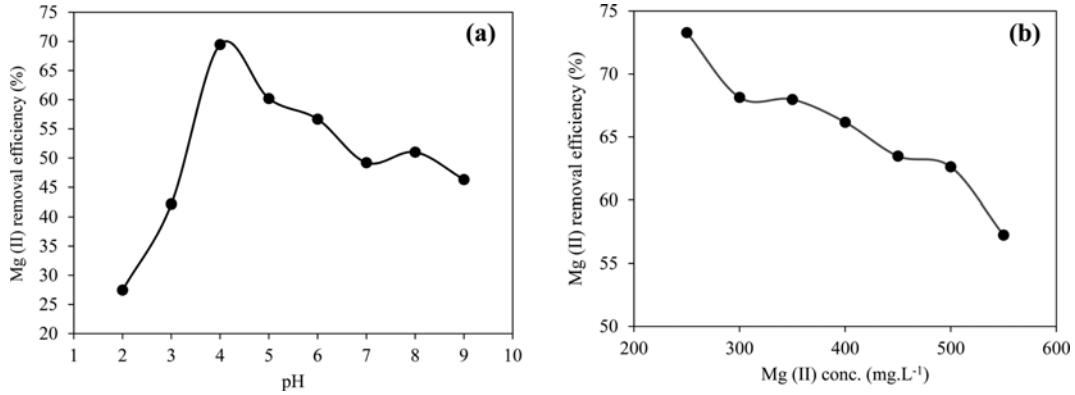

Fig. 6. Effect of (a) solution pH and (b) initial concentration of Mg (II) on the removal efficiency of Mg (II) on pristine bentonite. Conditions: particle size of bentonite: 88 μm, m: 1 g, V: 50 mL, t: 60 min, T: 30 °C, agitation speed: 100 rpm (In (a) Mg (II) conc.: 250 mg·L^{-1}, and in (b) pH: 4.00).

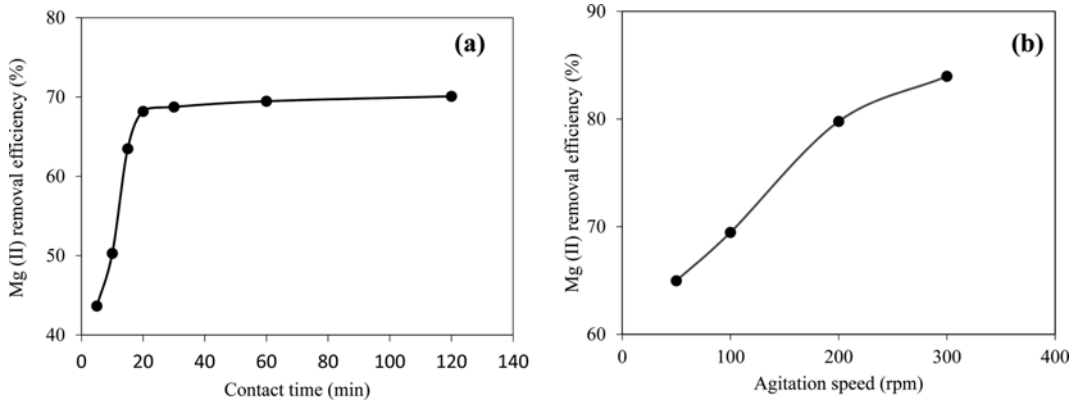

Fig. 7. Effect of (a) contact time and (b) agitation speed on removal efficiency of Mg (II) on pristine bentonite. Conditions: Mg (II) conc.: 250 mg·L^{-1}, particle size of bentonite: 88 μm, m: 1 g, pH: 4.00, V: 50 mL, T: 30 °C (In (a) agitation speed: 100 rpm and in (b) t: 60 min).

Mg (II) ion concentrations, more ions were available in order to occupy the active site of bentonite; accordingly, at higher concentration, the active sites of adsorbent were exhausted faster in comparison to lower concentrations [61].

4-4. Effect of Contact Time

Contact time play an important role in optimization of energy and processing period. The adsorption behavior of Mg (II) ions on bentonite was investigated as a function of contact time in the range of 5-120 min (Fig. 7(a)). The amount of ion removal increased from 43.65% to 70.09% at experiments conducted for 5 and 120 min time, respectively. The results indicate that Mg (II) removal using bentonite is a very fast process (especially at the beginning of adsorption), and it reached a maximum value in 20 min after mixing of bentonite and magnesium solution. After 20 min, no significant change in the Mg (II) removal was observed. This may be explained considering the availability of the large fraction of active sites at the surface of the adsorbent providing high tendency and the chance for firm adsorption of Mg ions. However, after almost full saturation of the surface sites, the only available opportunities remain within the internal structure of the adsorbent and within the pores which still enable adsorption to continue through intraparticle diffusion mechanism [40,62]. According to the results, 60 min was considered as the optimum equilibrium contact time for further experiments.

4-5. Effect of Agitation Speed

The agitation speed and turbulence of solution is one of the crucial parameters that can considerably influence the ion removal. Experimental data related to the effect of agitation speed on the removal efficiency are depicted in Fig. 7(b). According to the findings, the removal efficiency increased monotonically upon increase in the agitation speed. The removal efficiency of Mg (II) by bentonite reached its maximum value of 83.97% upon agitation at 300 rpm. The transfer of metal ions from liquid (water) to solid (adsorbent) phase faces resistance due to formation of boundary layer at the interphase of liquid-solid. Increasing the agitation speed led to a decrease of the boundary layer thickness and improved the ions transfer from liquid to solid phase [60]. In addition, higher agitation speed also provides more chance for the penetration of metal ions into the internal porous structure of the particles and thus enabling consumption of more active sites.

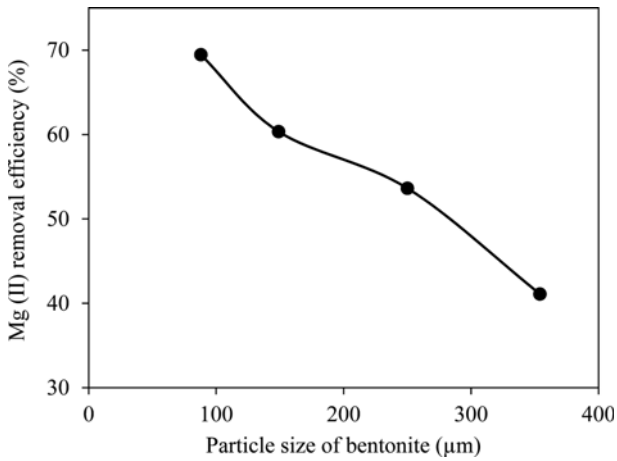

Fig. 8. Effect of particle size on removal efficiency of Mg (II) on pristine bentonite. Conditions: Mg (II) conc.: 250 mg·L^{-1}, m: 1 g, pH: 4.00, V: 50 mL, t: 60 min, T: 30 °C , agitation speed: 100 rpm.

4-6. The Effect Adsorbent Particle Size

Particle size is a well-known influential factor in adsorption processes. The effects of particle size of bentonite (varied from 88 to 354 μm) on Mg (II) adsorption are shown in Fig. 8. It is obvious that particles with smaller size offered higher removal efficiency. In other words, the removal efficiency of Mg (II) ions increased from 41.11% to 69.47% in adsorption by bentonite with particle sizes of 354 and 88 μm, respectively. This trend can be attributed to the tremendous effect of particle size and its increasing effect on the surface area and active sites [35]. According to these results, bentonite samples with particle size of 88 was selected for all other experiments.

5. Thermodynamic Studies

The effect of temperature on the removal efficiency of Mg (II) ions was investigated in the temperature range of 20-60 °C. According to Fig. 9(a), the removal efficiency of Mg (II) ions increased from 67.41% (at 20 °C) to 76.38% (at 60 °C), indicating that rise in temperature activated the metal ions for enhancing adsorption at the coordinating sites of the minerals [63]. Similar trends have

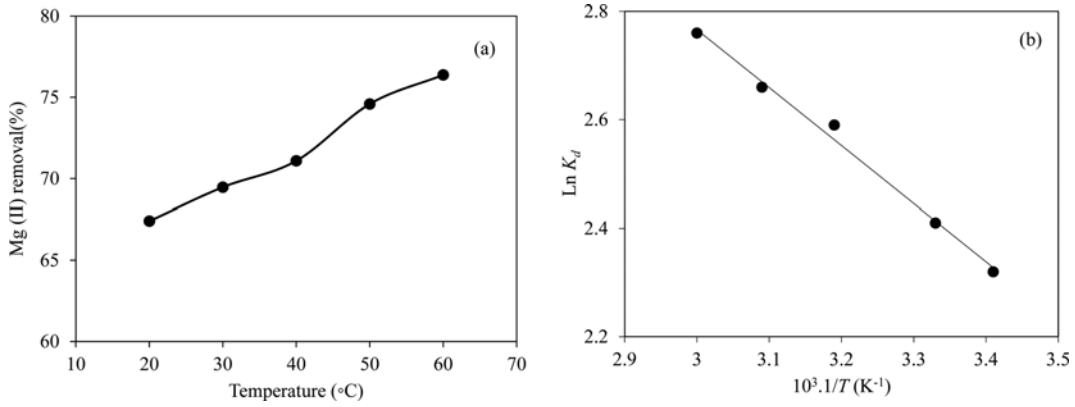

Fig. 9. (a) Effect of temperature on Mg (II) removal by pristine bentonite and (b) the plot of ln K_d versus 1/T for obtaining the thermodynamic parameters. Conditions: Mg (II) conc.: 250 mg·L^{-1}, particle size of bentonite: 88 μm, m: 1 g, pH: 4.00, V: 50 mL, t: 60 min, agitation speed: 100 rpm.

been reported for other heavy metal ions [35,40].

The feasibility of the adsorption process was determined using thermodynamic parameters, including the changes in Gibbs free energy (ΔG^o), enthalpy (ΔH^o) and entropy (ΔS^o). ΔG^o was calculated from the following equation [64]:

$$\Delta G^o = -RT\ln K_d \quad (4)$$

where R is the universal gas constant (8.314 J·mol^{-1}·K^{-1}), T is the temperature (K) and K_d is the distribution coefficient of adsorption calculated using the following equation [64]:

$$K_d = \frac{q_e}{C_e} \quad (5)$$

where q_e and C_e are the equilibrium concentration of Mg (II) ions on adsorbent (mg·L^{-1}) and in solution (mg·L^{-1}), respectively. K_d can be expressed in terms of change in enthalpy (ΔH^o) and entropy (ΔS^o) as a function of temperature according to the following equation:

$$\ln K_d = \frac{\Delta S^o}{R} - \frac{\Delta H^o}{RT} \quad (6)$$

The thermodynamic parameters of ΔH^o and ΔS^o were extracted from the slope and intercept of the plot of ln K_d versus 1/T, respectively, as shown in Fig. 9(b). The thermodynamic parameters for the bentonite-Mg (II) ion system are given in Table 3. The negative values of change in Gibbs free energy in the studied temperature range indicated that the adsorption process was feasible and spontaneous. Furthermore, the degree of spontaneity of the reaction increased with increasing temperature. The increase in adsorption with temperature may be attributed to the de-solvation of active sites on the adsorbent and, subsequently, decrease in the thickness of the surrounding boundary layer, and therefore the mass transfer resistance of adsorbate in the boundary layer decreases [40]. On the other hand, the positive sign of enthalpy change indicates an endothermic process. One possible explanation is that the metal ions are well solvated and have to lose part of their hydration sheath before being adsorbed and this requires energy. The energy of dehydration supersedes the exothermicity of the ions getting attach to the surface [65]. Furthermore, the positive value of adsorption entropy indicates that the adsorption process is irreversible and favors complexation and stability of sorption. The resultant effects of complex bonding and steric hindrance of the adsorbed species eventually lead to the increased enthalpy and entropy in the system [35].

6. Adsorption Isotherms

Adsorption isotherms are employed for gaining a better understanding of the mechanism of the adsorption and nature of the surface. Adsorption isotherms also provide useful information about the distribution of adsorbate molecules in solution (liquid phase) and on adsorbent (solid phase). In this study, the data obtained from the adsorption experiments were examined by using Langmuir, Freundlich and Dubinin-Radushkevich (D-R) isotherms, and discussions are provided in the following sections.

6-1. Langmuir Isotherm

The Langmuir model assumes that maximum adsorption correlates with a saturated monolayer of solute on the adsorbent surface with no lateral interaction between the adsorbed species [66]. The linear form of the Langmuir isotherm model can be presented as:

$$\frac{C_e}{q_e} = \frac{1}{q_0 K} + \frac{C_e}{q_0} \quad (7)$$

where q_e (mg·g^{-1}) is the amount of the metal ions adsorbed per unit mass of adsorbent, C_e (mg·L^{-1}) is the equilibrium metal ions concentration in the solution, q_0 (mg·g^{-1}) is the Langmuir constant

Table 3. Thermodynamic parameters for the system of Mg (II) and natural bentonite at various temperatures

ΔH^o (Kj·mol^{-1})	ΔS^o (j·mol^{-1}·K^{-1})	ΔG^o (Kj·mol^{-1})				
		293 K	303 K	313 K	323 K	333 K
9.13	50.40	−5.67	−6.14	−6.64	−7.14	−7.63

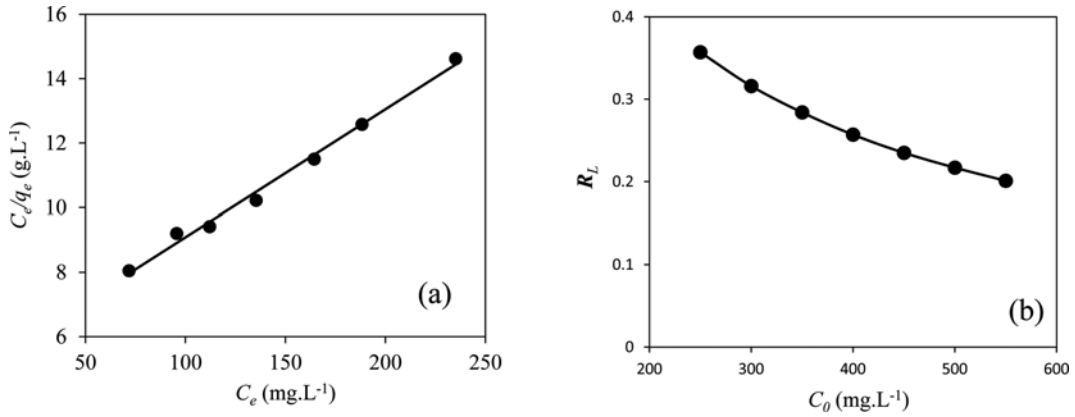

Fig. 10. (a) Linear plot of Langmuir isotherm for Mg (II) ion adsorption on natural bentonite at 30 °C (b) variation of separation factor (R_L) as a function of initial Mg (II) concentration.

Table 4. Langmuir, Freundlich and the D-R isotherm constants and correlation coefficients for adsorption of Mg (II) on pristine bentonite

Isotherm	Parameters
Langmuir	
q_0 (mg·g^{-1})	26.24
K (L·mg^{-1})	0.0072
R^2	0.992
Freundlich	
K_f (mg·g^{-1} (L$^{1/n}$·mg$^{-1/n}$)	0.9958
n	1.92
R^2	0.952
D-R	
β (mol^2·kJ^{-2})	0.0087
q_m (mol·g^{-1})	0.00238
E (kJ·mol^{-1})	7.58
R^2	0.983

related to the maximum monolayer adsorption capacity, and b (L·mg^{-1}) is the constant related to the free energy or net enthalpy of adsorption. The values of q_0 and K were obtained from intercept and slope of the linear plot of C_e/q_e versus C_e (Fig. 10(a)). The Langmuir model parameters and the statistical fits of the sorption data are given in Table 4. The linear plot of specific sorption (C_e/q_e) versus equilibrium concentration (C_e) shows that the adsorption of Mg (II) ions on bentonite obeys the Langmuir model. The essential features of the Langmuir isotherm can be expressed by dimensionless constant called equilibrium parameter or separation factor (R_L) which is defined as:

$$R_L = \frac{1}{1+KC_0} \tag{8}$$

where C_o is the initial concentration (mg·L^{-1}). There are four probabilities for the R_L value: for favorable adsorption, $0<R_L<1$; for unfavorable adsorption, $R_L>1$; for linear adsorption, $R_L=1$; and for irreversible adsorption, $R_L=0$ [66]. Accordingly, Fig. 10(b) indicates the variation of equilibrium parameter (R_L) with respect to initial Mg (II) ion concentration. The R_L values were in the range of 0-1 at 30 °C, showing that the adsorption of Mg (II) ions on bentonite is favorable in initial concentration range 250-550 mg·L^{-1}. Maximum sorption capacities according to the Langmuir constant (q_0) for adsorption of Mg (II) ions on various natural adsorbents are tabulated in Table 5 to allow comparison with the results from the present work [67].

Table 5. Maximum adsorption capacity of some adsorbents for magnesium ions removal from aqueous solution

Adsorbent	q_{max} (mg·g^{-1})	Ref.
Bentonite (natural) (B-N)	26.24	Present study
Calcined bentonite (B-C-400)	35.67	Present study
Microwave radiated zeolite (Z-R-15)	31.23	Present study
Chemically modified cellulose	13.5	[67]
Modified pumice	56.11	[3]

6-2. Freundlich Isotherm

The Freundlich isotherm model is valid for non-ideal and multilayer adsorption on heterogeneous surfaces with sites that have different energies of sorption and is expressed by the following linearized equation [64,66]:

$$\mathrm{Log}(q_e) = \mathrm{Log}(K_f) + \frac{1}{n}\mathrm{Log}(C_e) \tag{9}$$

where K_f and n are Freundlich constants related to adsorption capacity and adsorption intensity, respectively. The value of n varies with the heterogeneity of the adsorbent and for favorable adsorption process, the value of n should be higher than unity. The values of K_f and n (Table 4) were determined from the intercept and slope of linear plot of log (q_e) versus log (C_e) (Fig. 11(a)) and found to be 0.99 mg·g^{-1} and 1.92, respectively. The n value is higher than unity and therefore this system can be considered favorable for adsorption according to the Freundlich isotherm.

6-3. D-R Isotherm

The equilibrium data were also applied to the D-R model to determine the type of adsorption. This model enables prediction of energy of adsorption per unit of adsorbate and a maximum adsorption capacity of the adsorbent. The E value often varies from

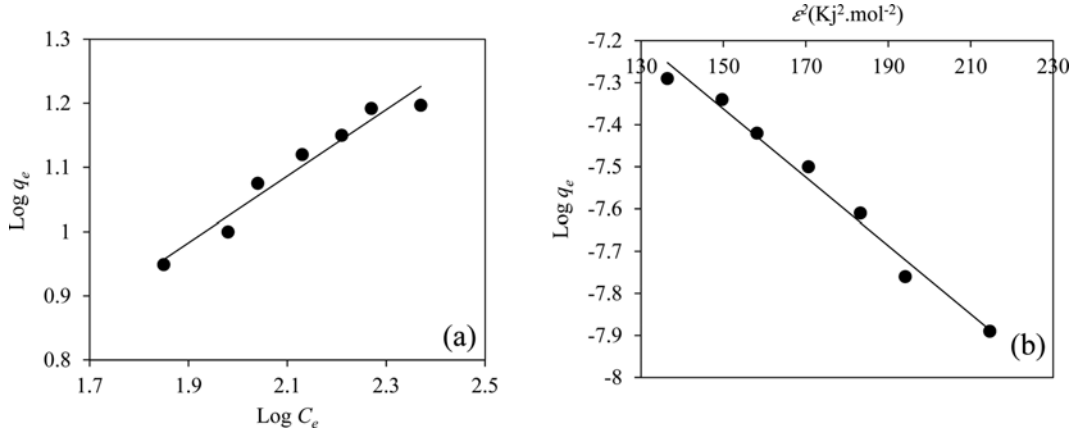

Fig. 11. (a) Linear plots of Freundlich isotherm of Mg (II) adsorption on pristine bentonite at 30 °C (b) D-R isotherm plot of Mg (II) adsorption on pristine bentonite at 30 °C.

1 to 8 kJ·mol^{-1} for physical adsorption and from 8 to 16 kJ·mol^{-1} for chemical adsorption [66]. The linear form of D-R isotherm is presented by the following equation [66]:

$$\ln q_e = \ln q_m - \beta\varepsilon^2 \quad (10)$$

where ε (Polanyi potential) is equal to RT ln (1+1/C_e), q_e is the amount of the solute adsorbed per unit natural bentonite (mol·g^{-1}), q_m the theoretical monolayer saturation capacity (mol·g^{-1}), C_e the equilibrium concentration of the solute (mol·L^{-1}), β the constant of the adsorption energy (mol^2·kJ^{-2}). β is related to mean adsorption energy (E, kJ·mol^{-1}) defined as:

$$E = \frac{1}{\sqrt{-2\beta}} \quad (11)$$

Values of q_m and β were obtained from the plot of ln q_e versus ε^2 (Fig. 11(b)), and are tabulated in Table 4. According to these data, E is 7.58 kJ·mol^{-1} for Mg (II) adsorption on natural bentonite. The value of E indicates occurrence of physical adsorption. The large difference between q_0 derived from the Langmuir and q_m from D-R isotherms may be due to the different definition of maximum adsorption capacity in two isotherms. In Langmuir isotherm, q_0 displays the maximum adsorption of adsorbate species at monolayer coverage, whereas q_m displays the maximum adsorption of adsorbate species at the total specific micropore volume of the adsorbent in D-R isotherm. Compared with the correlation coefficient value of the Langmuir isotherm, those of Freundlich isotherm and D-R isotherm were found less satisfactory (R^2<0.99).

7. Desorption and Regeneration

It is very important to regenerate the adsorbents for reusing and reducing the process cost. Regeneration of adsorbents was investigated by washing spent bentonite with 1 molar solutions of HNO_3, HCl and NaOH, as well as deionized H_2O. According to the results shown in Fig. 12, among the desorbing solutions used in the present study, HNO_3 could exhibit better performance. The yield is in the following order: HNO_3>HCl>NaOH>H_2O.

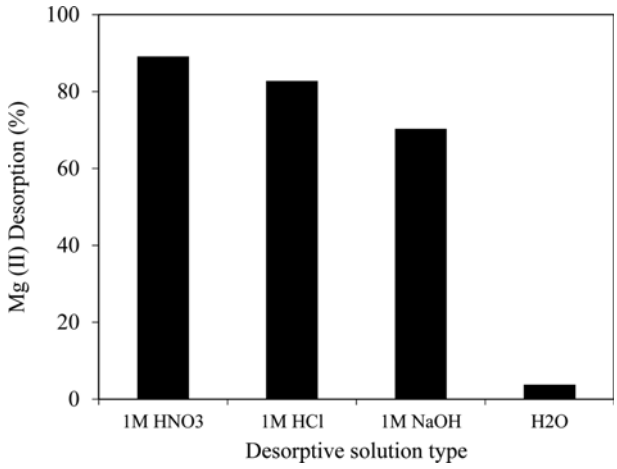

Fig. 12. Desorption yields of some desorptive solutions in the case of spent bentonite.

CONCLUSIONS

The properties and behavior of zeolite and bentonite for magnesium removal were improved through appropriate modification methods and investigation of process parameters. The experimental data demonstrated that selected inorganic adsorbents could be successfully used for the adsorption of magnesium from aqueous solutions. Acid and thermal modification of zeolite and bentonite resulted in significant enhancement in magnesium removal efficiency. Maximum removal efficiency was found 85.21% for the thermal-treated bentonite in furnace. Langmuir, Freundlich and Dubinin-Radushkevich (D-R) isotherms were used to represent the experimental data. The adsorption of magnesium was best represented by the Langmuir isotherm, which indicated a monolayer adsorption. R_L value for Langmuir and the n value for Freundlich isotherm indicated that Mg (II) ions were favorably adsorbed by natural bentonite. According to mean adsorption energy (E) obtained from the D-R isotherm, adsorption of Mg (II) ions onto natural bentonite was defined as physical. The negative ΔG^o values indicated that the adsorption of Mg (II) ions onto natural bentonite was feasible and spontaneous. Moreover, the positive value of ΔH^o confirmed the endothermic nature of adsorption. The positive values of ΔS^o suggested the increased randomness at the solid/

liquid interface during the adsorption of magnesium onto natural bentonite. With respect to experimental results and low cost of zeolite and bentonite, natural and modified inorganic adsorbent can be successfully used for effective removal of magnesium ions from aqueous solutions.

ACKNOWLEDGEMENTS

Authors would like to thank Iran Nanotechnology Initiative Council (INIC) for partial financial support rendered to this project.

REFERENCES

1. M. R. Awual, *Chem. Eng. J.*, **266**, 368 (2015).
2. A. Aghakhani, S. Mousavi, B. Mostafazadeh-Fard, R. Rostamian and M. Seraji, *Desalination*, **275**, 217 (2011).
3. M. N. Sepehr, M. Zarrabi, H. Kazemian, A. Amrane, K. Yaghmaian and H. R. Ghaffari, *Appl. Surf. Sci.,* **274**, 295 (2013).
4. F. Fu and Q. Wang, *J. Environ. Manage.*, **92**, 407 (2011).
5. M. R. Awual, *Chem. Eng. J.*, **300**, 264 (2016).
6. L. F. Greenlee, D. F. Lawler, B. D. Freeman, B. Marrot and P. Moulin, *Water Res.*, **43**, 2317 (2009).
7. S. Jamaly, N. N. Darwish, I. Ahmed and S. W. Hasan, *Desalination*, **354**, 30 (2014).
8. T. Jeppesen, L. Shu, G. Keir and V. Jegatheesan, *J. Cleaner Production*, **17**, 703 (2009).
9. J. Le Dirach, S. Nisan and C. Poletiko, *Desalination*, **182**, 449 (2005).
10. F. Fu and Q. Wang, *J. Environ. Manage.*, **92**, 407 (2011).
11. H. A. Abdulgader, V. Kochkodan and N. Hilal, *Sep. Purif. Technol.*, **116**, 253 (2013).
12. L. Birnhack and O. Lahav, *Water Res.*, **41**, 3989 (2007).
13. D. Muraviev, J. Noguerol and M. Valiente, *React. Funct. Polym.*, **28**, 111 (1996).
14. S. S. Hosseini and M. A. Alaei Shahmirzadi, *Ir. J. Chem. Eng.*, **13**, 91 (2015).
15. S. S. Hosseini, E. Bringas, N. R. Tan, I. Ortiz, M. Ghahramani and M. A. Alaei Shahmirzadi, *J. Water Process Eng.*, **9**, 78 (2016).
16. M. A. Alaei Shahmirzadi, S. S. Hosseini, G. Ruan and N. R. Tan, *RSC Adv.*, **5**, 49080 (2015).
17. V. K. Gupta, I. Ali, T. A. Saleh, A. Nayak and S. Agarwal, *RSC Adv.*, **2**, 6380 (2012).
18. A. Mittal, J. Mittal, A. Malviya and V. Gupta, *J. Colloid Interface Sci.*, **340**, 16 (2009).
19. M. R. Awual, *Chem. Eng. J.*, **289**, 65 (2016).
20. M. R. Awual, T. Yaita, S. A. El-Safty, H. Shiwaku, S. Suzuki and Y. Okamoto, *Chem. Eng. J.*, **221**, 322 (2013).
21. M. R. Awual, T. Yaita, H. Shiwaku and S. Suzuki, *Chem. Eng. J.*, **276**, 1 (2015).
22. V. Gupta and A. Nayak, *Chem. Eng. J.*, **180**, 81 (2012).
23. V. K. Gupta, R. Jain, A. Mittal, T. A. Saleh, A. Nayak, S. Agarwal and S. Sikarwar, *Mater. Sci. Eng.: C*, **32**, 12 (2012).
24. V. K. Gupta, R. Jain, A. Nayak, S. Agarwal and M. Shrivastava, *Mater. Sci. Eng.: C*, **31**, 1062 (2011).
25. S. Karthikeyan, V. Gupta, R. Boopathy, A. Titus and G. Sekaran, *J. Molecular Liquids*, **173**, 153 (2012).
26. A. Mittal, J. Mittal, A. Malviya and V. Gupta, *J. Colloid Interface Sci.*, **344**, 497 (2010).
27. M. Naushad, Z. ALOthman and H. Javadian, *J. Ind. Eng. Chem.*, **25**, 35 (2015).
28. M. Naushad, Z. ALOthman, M. Khan, N. ALQahtani and I. ALSohaimi, *J. Ind. Eng. Chem.*, **20**, 4393 (2014).
29. A. A. Alqadami, M. Naushad, M. A. Abdalla, T. Ahamad, Z. A. Alothman and S. M. Alshehri, *RSC Adv.*, **6**, 22679 (2016).
30. V. K. Gupta, S. Agarwal and T. A. Saleh, *J. Hazard. Mater.*, **185**, 17 (2011).
31. M. Naushad, T. Ahamad, G. Sharma, H. Ala'a, A. B. Albadarin, M. M. Alam, Z. A. ALOthmana, S. M. Alshehria and A. A. Ghfar, *Chem. Eng. J.*, **300**, 306 (2016).
32. G. Sharma, A. Kumar, M. Naushad, D. Pathania and M. Sillanpää, *J. Ind. Eng. Chem.*, **33**, 201 (2016).
33. G. Sharma, M. Naushad, A. Kumar, S. Devi and M. R. Khan, *Iranian Polym. J.*, **24**, 1003 (2015).
34. M. A. Tofighy and T. Mohammadi, *Desalination*, **268**, 208 (2011).
35. N. Karapinar and R. Donat, *Desalination*, **249**, 123 (2009).
36. A. S. Özcan and A. Özcan, *J. Colloid Interface Sci.*, **276**, 39 (2004).
37. T. K. Sen and D. Gomez, *Desalination*, **267**, 286 (2011).
38. E. L. Cooney, N. A. Booker, D. C. Shallcross and G. W. Stevens, *Sep. Sci. Technol.*, **34**, 2307 (1999).
39. S. Wang and Y. Peng, *Chem. Eng. J.*, **156**, 11 (2010).
40. S. Aytas, M. Yurtlu and R. Donat, *J. Hazard. Mater.*, **172**, 667 (2009).
41. L. Lei, X. Li and X. Zhang, *Sep. Purif. Technol.,* **58**, 359 (2008).
42. C. Bertagnolli, S. J. Kleinübing and M. G. C. Da Silva, *Appl. Clay Sci.*, **53**, 73 (2011).
43. T. Motsi, N. Rowson and M. Simmons, *Int. J. Min. Process.*, **92**, 42 (2009).
44. A. R. Kul and H. Koyuncu, *J. Hazard. Mater.*, **179**, 332 (2010).
45. S. Ü. Çelik, A. Bozkurt and S. S. Hosseini, *Progress in Polym. Sci.*, **37**, 1265 (2012).
46. S. S. Hosseini, *Membranes and Materials for Separation and Purification of Hydrogen and Natural Gas*, PhD Thesis, Department of Chemical and Biomolecular Engineering, National University of Singapore (2009).
47. A. R. Greenberg, E. Kujundzic, B. Krantz William, A. Yeo and S. S. Hosseini, *Determination of pore size in porous materials by evaporative mass loss*, US Patent, 20130042670 (2011).
48. S. S. Hosseini and T. S. Chung, *J. Membr. Sci.*, **328**, 174 (2009).
49. W. B. Krantz, A. R. Greenberg, E. Kujundzic, A. Yeo and S. S. Hosseini, *J. Membr. Sci.*, **438**, 153 (2013).
50. S. S. Hosseini and T. S. Chung, *Polymer blends and carbonized polymer blends*, US Patent 8,623,124 (2014).
51. S. Najari, S. S. Hosseini, M. Omidkhah and N. R. Tan, *RSC Adv.*, **5**, 47199 (2015).
52. S. S. Hosseini and S. Najari, in Polymeric Membranes for Gas and Vapor Separations, Nanostructured Polymer Membranes: Applications Vol. 2, P.M. Visakh and N. Olga, Wiley (2016).
53. S. S. Hosseini, S. M. Roodashti, P. K. Kundu and N. R. Tan, *Can. J. Chem. Eng.*, **93**(7), 1275 (2015).
54. S. S. Hosseini, J. A. Dehkordi, P. K. Kundu, *Korean J. Chem. Eng.* (2016), DOI:10.1007/s11814-016-0198-z.
55. H. Faghihian and M. Nejati-Yazdinejad, *Adsorpt. Sci. Technol.*, **27**, 107 (2009).
56. H. Kazemian, H. Modarress, M. Kazemi and F. Farhadi, *Powder*

Technol., **196**, 22 (2009).
57. M. Hayati-Ashtiani, *Part. Sci. Technol.*, **31**, 419 (2013).
58. H. Kurama, A. Zimmer and W. Reschetilowski, *Chem. Eng. Technol.*, **25**, 301 (2002).
59. Z.-r. Liu and S.-q. Zhou, *Process Safety Environ. Protection*, **88**, 62 (2010).
60. D. Xu, X. Tan, C. Chen and X. Wang, *Appl. Clay Sci.*, **41**, 37 (2008).
61. D. Thakre, S. Rayalu, R. Kawade, S. Meshram, J. Subrt and N. Labhsetwar, *J. Hazard. Mater.*, **180**, 122 (2010).
62. W. Plazinski and W. Rudzinski, *J. Phys. Chem. C*, **113**, 12495 (2009).
63. V. J. Inglezakis, M. A. Stylianou, D. Gkantzou and M. D. Loizidou, *Desalination*, **210**, 248 (2007).
64. H. B. Senturk, D. Ozdes, A. Gundogdu, C. Duran and M. Soylak, *J. Hazard. Mater.*, **172**, 353 (2009).
65. R. Naseem and S. Tahir, *Water Res.*, **35**, 3982 (2001).
66. H. Zheng, D. Liu, Y. Zheng, S. Liang and Z. Liu, *J. Hazard. Mater.*, **167**, 141 (2009).
67. O. Karnitz, L. V. A. Gurgel and L. F. Gil, *Carbohydrate Polymers*, **79**, 184 (2010).